Global and Planetary Change 177 (2019) 27–38

Contents lists available at ScienceDirect

Global and Planetary Change

journal homepage: www.elsevier.com/locate/gloplacha

NDVI indicated inter-seasonal non-uniform time-lag responses of terrestrial vegetation growth to daily maximum and minimum temperature

Youyue Wen[a,b], Xiaoping Liu[a,*], Jian Yang[b], Kui Lin[b], Guoming Du[a]

[a] School of Geography and Planning, Sun Yat-sen University, NO.135 West Xingang RD., Guangzhou 510275, PR China
[b] South China Institute of Environmental Science, Ministry of Ecology and Environment, NO.18 Ruihe RD., Guangzhou 510535, PR China

ARTICLE INFO

Keywords:
Asymmetric warming
Time-lag effects
Tmax
Tmin
Vegetation types
Climate change

ABSTRACT

Climate warming exhibits asymmetric patterns over a diel cycle, with the trend of daily minimum temperature (Tmin) exceeds that of daily maximum temperature (Tmax), which is expected to significantly affect terrestrial vegetation growth. To date, many studies have documented the instantaneously asymmetric impacts of Tmax and/or Tmin on terrestrial ecosystems, but little is known about the non-uniform time-lag effects of Tmax and/or Tmin on vegetation growth. Using monthly datasets of normalized difference vegetation index (NDVI) as the proxy for vegetation vigor and the accumulated Tmax and Tmin on representatives of asymmetric warming, we quantitatively investigated the inter-seasonal non-uniform time-lag effects of Tmax and/or Tmin on terrestrial vegetation growth from 1982 to 2014 by applying partial correlation and time-lag analyses. Our results indicate that both Tmax and Tmin have significant time-lag effects on vegetation growth that exhibit spatial heterogeneities; the same vegetation type exhibits distinguished asymmetric responses to Tmax vs. Tmin; and different vegetation types respond to Tmax and/or Tmin with diverse time-lag effects; the overall average lagged times of Tmax and Tmin on vegetation growth were 1.68 ± 1.05 months and 1.45 ± 0.96 months, respectively; terrestrial vegetation growth correlates with Tmax reversely against Tmin over most regions and vegetation types. This study provided new insights into the non-uniform responses of vegetation to asymmetric warming. Moreover, our findings highlight the urgency of the currently used climate-vegetation models to consider the non-uniform time-lag effects found in this study so as to improve their performances in future investigation of vegetation-climate interactions.

1. Introduction

The terrestrial ecosystem has undergone continual warming since the 1950s (IPCC, 2014; Vose et al., 2005), which is characterized not only by an increase in the daily mean temperature but also by a noticeable asymmetric pattern in the warming trend over a diel cycle. Namely, a greater warming tendency in daily minimum temperature (Tmin) than in daily maximum temperature (Tmax) – a phenomenon commonly known as asymmetric warming (Peng et al., 2013). The causes behind the asymmetric warming are uncertain, but it suggests that the increases in cloud cover is the probable cause of the observed diurnal asymmetric warming (Flower and Gonzalez-Meler, 2015; Weber et al., 1994). Projections suggest this asymmetric warming is likely to be enhanced in following decades (IPCC, 2014; Zhou et al., 2009). Tmax appears during the daytime, and increase in Tmax strongly affects the diurnal plant photosynthesis; Tmin, however, occurs in the nighttime, and larger Tmin greatly influences nocturnal plant respiration (Anderegg et al., 2015; Chen et al., 2017; Peng et al., 2013). Therefore, the ongoing enhanced warming asymmetry is expected to exert significant impacts on the structures, functions and services of terrestrial vegetation and even entire ecosystems (Gordon, 2008; Peng et al., 2013; Su et al., 2015).

A growing body of literature has documented the significant effects of Tmax and Tmin on terrestrial vegetation. For instance, the Tmax has been found to positively correlate with the normalized difference vegetation index (NDVI) of most vegetation types in wet and cool regions, but to negatively correlate with the NDVI in dry temperate zones; however, Tmin has negative associations with the NDVI of plants growing in boreal ecosystems (Peng et al., 2013). These non-uniform impacts are characterized by seasonal distinctions (Tan et al., 2014), i.e. the spring has larger vegetated areas covered by positive correlations between Tmax and NDVI compared to summer and autumn; however, summer, rather than spring or autumn, has the strongest negative correlations between Tmax and NDVI in temperate dry regions; and the autumn NDVI has the weakest positive relationship with Tmin over most temperate regions in the Northern Hemisphere. The vegetation productivities were greatly influenced by Tmax and Tmin, which varies

* Corresponding author.
E-mail address: liuxp3@mail.sysu.edu.cn (X. Liu).

https://doi.org/10.1016/j.gloplacha.2019.03.010
Received 25 February 2018; Received in revised form 10 March 2019; Accepted 14 March 2019
Available online 16 March 2019
0921-8181/ © 2019 Elsevier B.V. All rights reserved.

by region and season as well (Su et al., 2015; Tan et al., 2014; Xia et al., 2014). For example, on the one hand, Tmax can enhance the carbon gains in plants at high latitudes and elevations (i.e. the polar, boreal zone and the Tibetan Plateau), especially in spring and autumn, on the other hand, it can also suppress the carbon uptakes in most of the other regions, especially in summer; however, the reverse situation occurs in the effects of Tmin on vegetation productivity over the most terrestrial surfaces (Tan et al., 2014; Xia et al., 2014). Additionally, conflicting results have been found in the impacts of Tmax and/or Tmin on the physiological vegetation processes and phenology, for instance, Anderegg et al. (2015) reported that Tmin dominates the terrestrial carbon release in tropical zones likely through enhancing dark respiration; however, Wan et al. (2009) found that Tmin could result in a minor carbon sink in a temperate steppe ecosystem by consuming leaf carbohydrates and stimulating the following day-time photosynthesis in plants; Xia and Wan (2012) found that on semi-arid grasslands, Tmin, but not Tmax, showed closer association with plant phenology; furthermore, Wang et al. (2017) also found that Tmin dominated the spatiotemporal patterns of deciduous broadleaved forest phenology changes; inversely, Piao et al. (2015) reported that green plant leaf onset was triggered by Tmax rather than Tmin in the Northern Hemisphere.

These aforementioned studies have demonstrated the complex interactions between asymmetric warming and terrestrial plant growth, but they primarily focused on the simultaneous interactions, which means that they paid little attention to the important fact that previous climatic conditions (the asymmetric warming, in particular, in this study) may also have massive impacts on the current green plant growth – a phenomenon commonly referred as time-lag effects (Wu et al., 2015). Therefore, the uncertainties of their results might be enhanced. There are abundant evidences that have corroborated the widespread spatio-temporal existence of time-lag effects of antecedent temperature on vegetation growth. For instance, Braswell et al. (1997) found that a warm temperature anomaly in terrestrial ecosystems is accompanied by an NDVI anomaly with a 2-year lag; Piao et al. (2003) reported that there is nearly a 3-month lag in the NDVI responses to temperature in China; Mulder et al. (2016) found that warmer summer temperatures in the prior 1 or 2 years can negatively affect the flowering phenology of a subarctic plant community; and studies by Wu et al. (2015) and Xu et al. (2014) indicated that time-lag effects of temperature on vegetation growth are various among vegetation types and spaces.

These temperature-induced time-lag effects benefit the growth of green plants, as they buffer green plants from direct, adverse impacts from temperature anomalies and provided them a certain time interval to recover as before. Therefore, the time-lag effects have a great significance on plant growth and terrestrial ecosystem balance (Sherry et al., 2008; Vicente-Serrano et al., 2013; Wiegand et al., 2004). Furthermore, ascertaining the time-lag effects of ambient temperatures on vegetation growth and understanding their mechanisms is important for environment management (Braswell et al., 1997; Mulder et al., 2016; Sherry et al., 2008; Zhang et al., 2015), as we can take full response measures, in advance, when an anomalous temperature behavior is forecast. For example, to minimize the damages in roots and burgeen and the possible losses in harvest latter, farmers can put up a tent for tender plants before a coming heavy spring frost. Therefore, under the background of increasing asymmetric warming, it's of great importance and urgency to assess the time-lag effects of Tmax and Tmin on terrestrial vegetation growth, and knowledge of such time lags allows us to better understand the interactions between climate warming and vegetation growth.

Currently, great advances have been made in remote-sensing technology and theory, which expand the opportunities for timely monitoring of vegetation dynamics at regional to global scales (Shen et al., 2015; Tucker et al., 2005; Zeng et al., 2013). Remotely sensed NDVI, a vegetation index calculated as the difference between near-infrared and red reflectance values that are normalized over the sum of the two (Eidenshink and Faundeen, 1994), has been widely used as a proxy for the changes in terrestrial vegetation because NDVI shows close correlations with vegetation properties, such as the leaf area index (LAI), photosynthetic capacity, chlorophyll concentration in leaves and net vegetation productivity (NPP) (Nemani et al., 2003; Potter et al., 2012; Turner et al., 2006; Zhu et al., 2013). The NDVI ranges from −1 to 1, with larger positive NDVI values indicating higher vegetation coverage and stronger vegetation activity, and zero or negative values representing bright, non-vegetation surfaces, such as barren surfaces (rock or soil) or areas covered by water, snow, ice or clouds. NDVI has proven to be an effective medium for detecting and quantifying plant responses to environmental change (Dutta et al., 2015; Peng et al., 2013; Wu et al., 2015; Zeng et al., 2013). Increasing studies (Peng et al., 2013; Tan et al., 2014; Zeng et al., 2013) have documented how NDVI helps us to understand the interactions between Tmax and/or Tmin and vegetation variations, but the time-lag effects of NDVI responses to Tmax and/or Tmin have been minimally considered. Therefore, it is possible and necessary to study the lagged impacts of vegetation growth in response to Tmax and/or Tmin by using NDVI.

In summary, the simultaneous plant responses to Tmax and/or Tmin have been well documented, but the time-lag effects of Tmax and/or Tmin on terrestrial vegetation variations are not yet well understood. Therefore, we theorized that the Tmax and/or Tmin have significant non-uniform time-lag effects on the vegetation growth and focused on the following aims:

1) Quantifying the lagged time intervals of Tmax and/or Tmin on plant growth;
2) Disentangling the correlations between plant growth and Tmax and/or Tmin.

To do this, we used the changes in NDVI to represent the variations in vegetation growth, and we accumulated the monthly Tmax and Tmin to represent the condition of asymmetric warming (i.e. asymmetric temperature warming trend in Tmax and Tmin); then, we calculated the partial correlation coefficients (PR) between NDVI and Tmax and/or Tmin by applying partial correlation and time-lag analyses; after that, we obtained the optimal time lag (OTL) of Tmax and/or Tmin on vegetation and the optimal PR (OPR) between them; finally, the frequency and magnitude of the resulting OTL and OPR were further analyzed for different vegetation types.

2. Materials and methods

2.1. Global datasets

2.1.1. GIMMS NDVI dataset

The 3rd generation NDVI, version of the 1st (NDVI.3 g.v1), that was produced by the Global Inventory Monitoring and Modeling Studies (GIMMS) program was used for the present study. As the longest continuous temporal series of remote sensing based vegetation index data, the NDVI.3 g.v1 is one of the most commonly used datasets for monitoring long-term vast vegetation dynamic studies. The NDVI.3 g.v1 was based on NOAA's Advanced Very High Resolution Radiometer (AVHRR) sensors, it includes continuous monthly datasets from Jul. 1981 to Dec. 2015 and was provided with following attributes: a spatial resolution of 1/12 deg. and a 15-day interval (Tucker et al., 2005). The maximum value composite (MVC) method was applied on the original time series of NDVI.3 g.v1 to construct monthly NDVI datasets. Furthermore, we averaged the resulting monthly NDVI to 0.5° × 0.5° (Peng et al., 2013; Wu et al., 2015) to match the spatial resolution of climate datasets (hereafter “NDVI”).

2.1.2. Climate dataset

Five climatic datasets from Jan. 1982 to Dec. 2014 were used in this study, including the monthly average, maximum and minimum

temperature (Tavg, Tmax and Tmin), total precipitation (PRCP) and total downward shortwave solar radiation data (SW). All of them possess the attributes of monthly temporal resolution and 0.5° spatial resolution. The first four of these datasets originated from the time-series products (version TS3.24) provided by the Climatic Research Unit (CRU), in which additional updates were made to earlier products, such as the essential corrections to the precipitation errors in Cherrapunji and additions of new meteorological stations for Tavg, Tmax and Tmin (Harris et al., 2014). The SW originated from Princeton Global Forcings, version 2 (PGF.v2), which was created by the Terrestrial Hydrology Research Group at Princeton University. The PGF.v2 is a combination of reanalysis datasets from the National Centers for Environmental Prediction (NCEP) and the National Center for Atmospheric Research (NCAR), in which the known errors of solar radiation, i.e., the spatio-temporal disaggregation and trend biases etc., were carefully corrected using observation-based datasets and probability-weighted scaling methods (Sheffield et al., 2006).

2.1.3. Vegetation map

The University of Maryland created a 1 km land cover map from the AVHRR imageries (from Apr.1992 to Mar.1993) using a classification tree algorithm (Hansen et al., 2000). This thematic map has an overall accuracy between 81.4 and 90.3% and was further re-processed into 0.25°, 0.5° and 1.0° maps using a weighted-resampling method (Defries and Hansen, 2010) with the greatest dominance land cover type assigned in each pixel. These products have been effectively applied in previous global vegetation monitoring studies (Defries and Hansen, 2010; Nemani et al., 2003; Zhou et al., 2003). To avoid uncertainties resulted from different satellite sensors, though there are many newer and better vegetation maps, we decided to use the AVHRR-based vegetation map. Besides, to maintain a spatial resolution consistent with the NDVI and climate datasets, the 0.5° map (Fig. 1) was obtained in this study to specify the different vegetation types.

2.2. Accumulated daily maximum and minimum temperature

Former studies (Braswell et al., 1997; Musau et al., 2016; Sherry et al., 2008; Wu et al., 2015) have mostly considered the previous climatic condition at only one point in time when studying the time-lag effects of antecedent climatic factors on present plant growth. That is to say, suppose a climatic factor has a time-lag effect of 3 months on vegetation growth in the present month, these studies have only focused on the associations between the climatic condition of 3 months ago and the vegetation status in the present month, without considering the climatic conditions of the previous month and 2 months ago, which may also have significant impacts on the vegetation growth in the present month. Consequently, these studies ignored the important fact that the growth of green plants is probably influenced by the cumulative effects resulting from antecedent, ambient climatic conditions over a period time (Peng et al., 2010; Zeng et al., 2013). We tested this speculation (Figs. S1–S2) and found that additional consideration of the cumulative effects from ambient temperature (indicated by accumulated temperature (AT) (Zeng et al., 2013)) could significantly increase the areas covered by significant determination coefficient (R^2) values between accumulated temperature factors and NDVI (comparing Fig. S1.a with Fig. S1.b and comparing Fig. S2.a with Fig. S2.b). What's more, compared with the non-accumulated monthly Tmax, the accumulated monthly Tmax (ATmax) has closer associations with NDVI and the R^2 between them were increased by 0.08 at a global scale (Fig. S1.c), similarly, the R^2 between the accumulated monthly Tmin (ATmin) and NDVI were increased by 0.03 than that between the non-accumulated monthly Tmax and NDVI (Fig. S2.c). This means that temperature has significant cumulative effects on the vegetation growth, and the AT can better explanate and fit the variations of vegetation growth than non-accumulated temperature does.

AT is the summation, expressed in degrees, by which the real air temperature rises above or falls below a given standard temperature (T_{base}) over a particular period, i.e., in hours, months, seasons etc. In

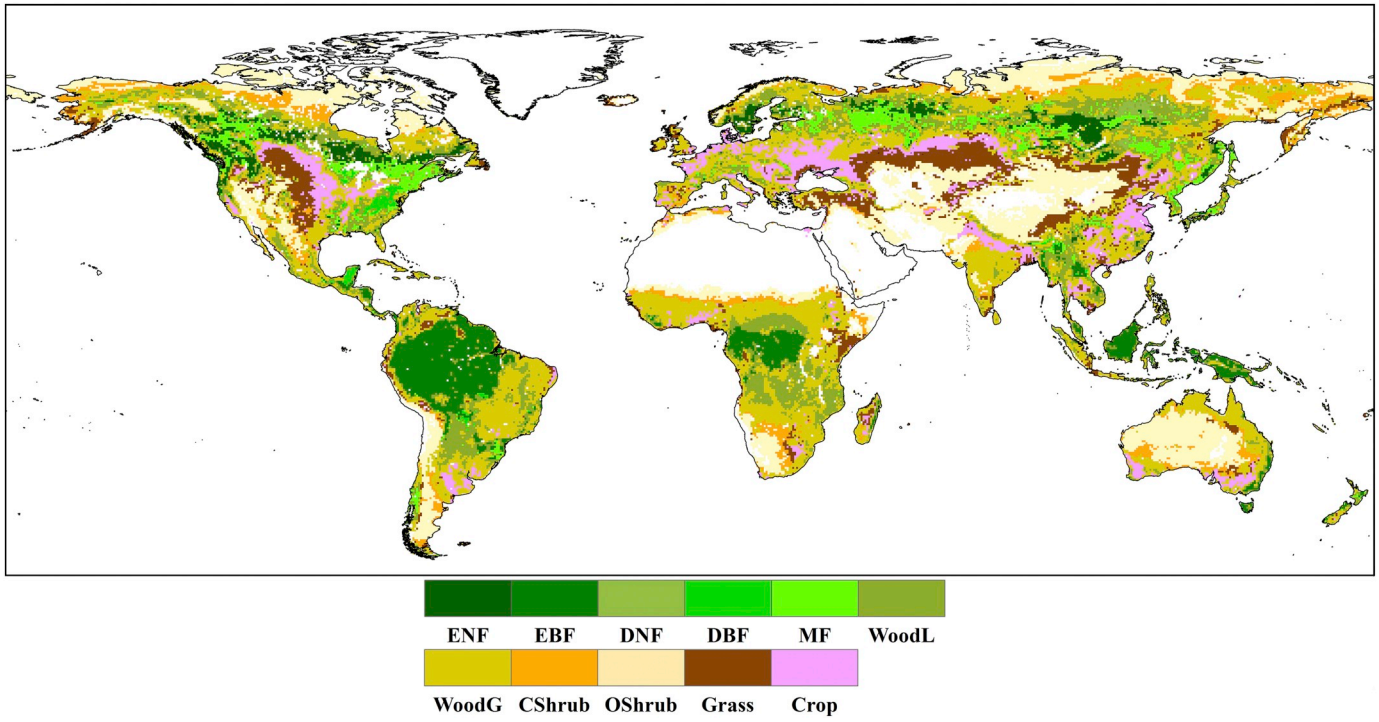

Fig. 1. The global land cover classifications (0.5°, 1992–1993) by the University of Maryland. In this map, each pixel assigned the cover type with the greatest dominance. Evergreen Needleleaf Forest (ENF), Evergreen Broadleaf Forest (EBF), Deciduous Needleleaf Forest (DNF), Deciduous Broadleaf Forest (DBF), Mixed Forest (MF), Woodland (WoodL), Wooded Grassland (WoodG), Closed Shrubland (CShrub), Open Shrubland (OShrub), Grassland (Grass) and Cropland (Crop). The definitions for these land cover types were provided in Table S1. The white area represents water, bare ground and permafrost horizon.

this study, the ATmax and ATmin were computed as in Eqs. (1) and (2) to represent the conditions of asymmetric warming. It deserves mentioning that AT only makes sense until a T_{base} is given; following previous studies (Anandhi, 2016; Garcia-Mozo et al., 2000; Piao et al., 2015), 0 °C was chosen here as the T_{base}. Furthermore, we specified the accumulation period as the lagged duration that Tmax and Tmin may exhibit on vegetation growth. Previous studies have shown the time lags at the monthly scale of the temperature on vegetation growth to generally be shorter than a quarter (Musau et al., 2016; Piao et al., 2003; Wang et al., 2009; Wu et al., 2015); therefore, in the present study, we considered the time lags for 0–3 months. Last but not least, following previous study (Garcia-Mozo et al., 2000), we assumed there is no addition to the ATmax or ATmin when monthly Tmax or Tmin was lower than T_{base}; therefore, ATmax and ATmin are non-negative parameters.

$$\mathrm{ATmax(m,i)} = \sum_{k=0}^{k=i} (\mathrm{Tmax}(m-k) - T_{base})\,(0 \le k \le i \le 3) \quad (1)$$

$$\mathrm{ATmin(m,i)} = \sum_{k=0}^{k=i} (\mathrm{Tmin}(m-k) - T_{base})\,(0 \le k \le i \le 3) \quad (2)$$

where the m is the month series from Jan. 1982 to Dec. 2014; the i is the supposed lagged duration (0–3 months); the k is the time scale prior to the present month m; and T_{base} equals 0°C. As an example, we computed the ATmax of Mar. 1982 with a time lag of 2 months ($\mathrm{ATmax}_{(Mar.\ 1982,2)}$) in the following steps:

a) Calculate the difference of maximum temperature in Mar. 1982 ($\mathrm{DTmax}_{Mar.\ 1982}$), Feb. 1982 ($\mathrm{DTmax}_{Feb.\ 1982}$) and Jan. 1982 ($\mathrm{DTmax}_{Jan.\ 1982}$) with reference to T_{base}.

$$\mathrm{DTmax}_{Mar.1982} = \mathrm{Tmax}_{Mar.1982} - T_{base} \quad (3)$$

$$\mathrm{DTmax}_{Feb.1982} = \mathrm{Tmax}_{Feb.1982} - T_{base} \quad (4)$$

$$\mathrm{DTmax}_{Jan.1982} = \mathrm{Tmax}_{Jan.1982} - T_{base} \quad (5)$$

b) Combine the temperature differences.

$$\mathrm{ATmax}_{(Mar.1982,2)} = \mathrm{DTmax}_{Mar.1982} + \mathrm{DTmax}_{Feb.1982} + \mathrm{DTmax}_{Jan.1982} \quad (6)$$

2.3. Partial correlation analyses

Partial correlation is a statistical measure of the direction and strength of a linear relationship between an independent variable and a dependent one (X, Y), while eliminating the disturbed impacts from one or more covariates (Z = [Z_1, Z_2…, Z_n]). The resulting partial correlation coefficient (PR) statistically ranges from −1 to +1, wherein the negative (positive) values denote negative (positive) correlations and the value of 0 represents no linear correlations. Here, we applied partial correlation analyses to acquire the correlations between NDVI and ATmax (or ATmin) (Peng et al., 2013) as in Eq. (7). Following some previous studies (Piao et al., 2007; Wu et al., 2015), the statistical analyses in the present study were based on the vegetation growing season, which was defined as the months when Tavg was greater than freezing (0 °C) and the NDVI was larger than 0.2. So only the monthly vegetated and climatic data that fell within the vegetation growing season were included into the regression. The spatial distribution of annual mean growing season length in months during 1982–2014 were show in Fig. S3. To minimize the possible spurious results from seasonal cycles and/or temporal autocorrelation of vegetation and climatic time series, we linearly detrended vegetation and all relevant climatic variables before any statistical analyses (Peng et al., 2013; Tan et al., 2014).

$$R_{X,Y|Z} = \frac{R_{XY} - R_{XZ} * R_{YZ}}{\sqrt{(1 - R_{XZ}^2) * (1 - R_{YZ}^2)}} \quad (7)$$

where X, Y and Z refer to NDVI, ATmax (or ATmin) and [ATmin, PRCP, SR] (or [ATmax, PRCP, SR]); the $R_{X,\ Y|Z}$ represents the PR between X and Y while controlling for the covariates (Z = [Z_1, Z_2…, Z_n]); and the R_{XY}, R_{YZ} and R_{XZ} are the regular correlation coefficients among X, Y and Z.

2.4. Time-lag effects analyses

In this study, the time-lag effects referred in particular to those of asymmetric warming on vegetation growth. There are two significant elements of the time-lag effects of asymmetric warming on terrestrial vegetation, one is the lagged time interval that the impacts of asymmetric warming may last on vegetation growth; the other is the correlation between the asymmetric warming and vegetation growth under this lagged time interval. We performed time-lag effects analyses as following steps: first, we assumed that certain lagged intervals (0 ≤ k ≤ 3 months) are exhibited in the effects of asymmetric warming on vegetation growth; then, at each supposed time lag, we obtained the accompanying PR (PR_0, PR_1, PR_2 and PR_3) between ATmax/ATmin and NDVI; finally, the PR (PR_k, 0 ≤ k ≤ 3) when it reached its maximum determination coefficient (PR_k^2), was taken as the optimal PR (OPR, Eq. (8)) between ATmax/ATmin and NDVI, and the k was considered to be the optimal time lag (OTL, Eq. (9)) for NDVI responses to ATmax/ATmin (Wu et al., 2015).

$$\mathrm{OPR} = PR_k,\ when\ PR_k^2 = Maximum\{PR_0^2, PR_1^2, PR_2^2, PR_3^2\}(0 \le k \le i \le 3) \quad (8)$$

$$\mathrm{OTL} = \mathrm{k},\ when\ PR_k^2 = Maximum\{PR_0^2, PR_1^2, PR_2^2, PR_3^2\}(0 \le k \le i \le 3) \quad (9)$$

3. Results

3.1. Time lags of NDVI responses to asymmetric warming

We obtained the spatial distributions of the OTL of inter-seasonal NDVI responses to ATmax (Fig. 2.a) and ATmin (Fig. 2.b) and the differences between them (Fig. 2.c). Results show that the average OTL of the NDVI responses to ATmin (1.68 ± 1.05 months) were near 0.23 months longer than the responses to ATmax (1.45 ± 0.96 months) at a global scale. According to Fig. 2.a-b (see also in Figs. S4.a-b and S5.a-b), the inter-seasonal NDVI variations have short time-lag responses to both ATmax and ATmin over the mid-high northern latitudes (> 45°N); in contrast, the NDVI in semi-arid and arid regions, such as the deserts in Australia and the Deccan Plateau, responds to asymmetric warming with a distinctly high lagged time. Fig. 2.d-e demonstrates that only small proportions of the global land area show no time lag in the responses of NDVI to ATmax (16.44%) and ATmin (17.04%); furthermore, the pixels that are covered by a 3-month lagged duration account for a larger percentage in the NDVI responses to ATmin (27.14%) than to ATmax (17.56%), which was confirmed again in the results in Figs. S4.d-e and S5.d-e. Fig. 2.d shows that the grids covered by a 1-month delay account for 39.48% of the global grids, followed by a 2-month time lag that comprises 26.11%, which implies that most terrestrial vegetation growth (65.59%) inclines to respond to ATmax with time-lag effects up to 1–2 months (see also in Figs. S4.d and S5.d). As shown in Fig. 2.e, the frequencies of different lagged time scales of NDVI to ATmin are distributed evenly, with the largest frequency (30.71%) appearing in the 2-month time lag.

According to Fig. 2.c and f, the regions with longer OTL in NDVI responses to ATmax than to ATmin (brown areas in Fig. 2.c) account for up to 31.00% of the total areas, which is approximately 18.57% larger than the reverse situation (blue areas in Fig. 2.c); these results suggest that there are a considerable amount of vegetation pixels (43.44%) that are characterized by unequal OTL in NDVI responses to ATmax vs. ATmin (see also in Figs. S4.c and f and S5.c and f). Linking Fig. 2.c and

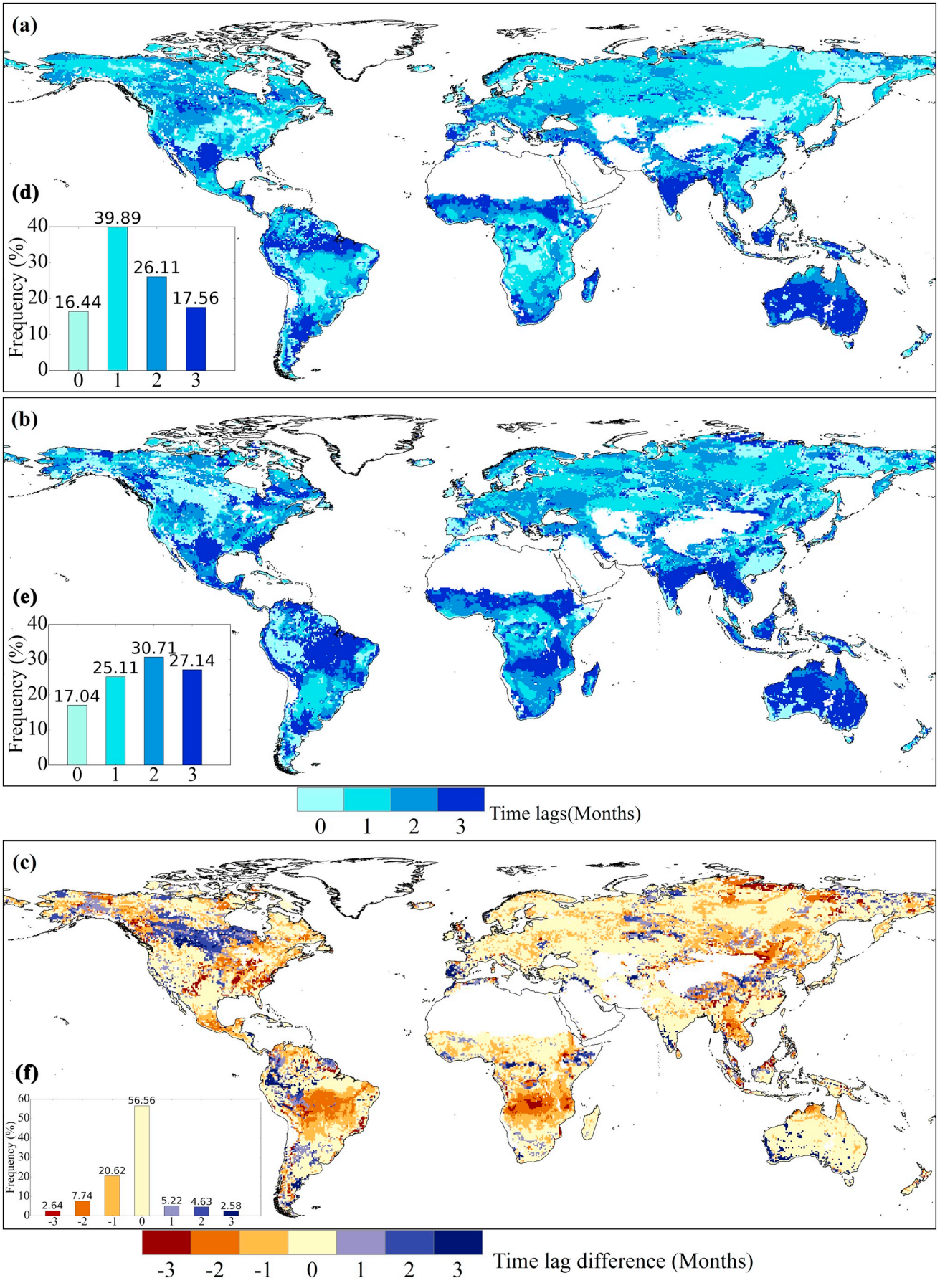

(caption on next page)

Fig. 2. Spatial distributions of OTL of NDVI responses to ATmax (a) and ATmin (b) and the OTL difference (c) of the result in Fig. 2.a to that in Fig. 2.b from 1982 to 2014. The inset bar charts of Fig. 2.d-f show the frequency distributions of the grids with different lagged values in corresponding maps. The negative values in Fig. 2.c represent the NDVI responses to ATmax that exhibit shorter time lags than to ATmin (brown areas), whereas the positive values denote the NDVI responses to ATmax that exhibit longer time lags than to ATmin (blue areas), and the zeros represent the NDVI response to ATmax and ATmin with equal lag time (pale yellow areas). White areas represent places with no data or with no significant correlations ($p > .05$). (For interpretation of the references to colour in this figure legend, the reader is referred to the web version of this article.)

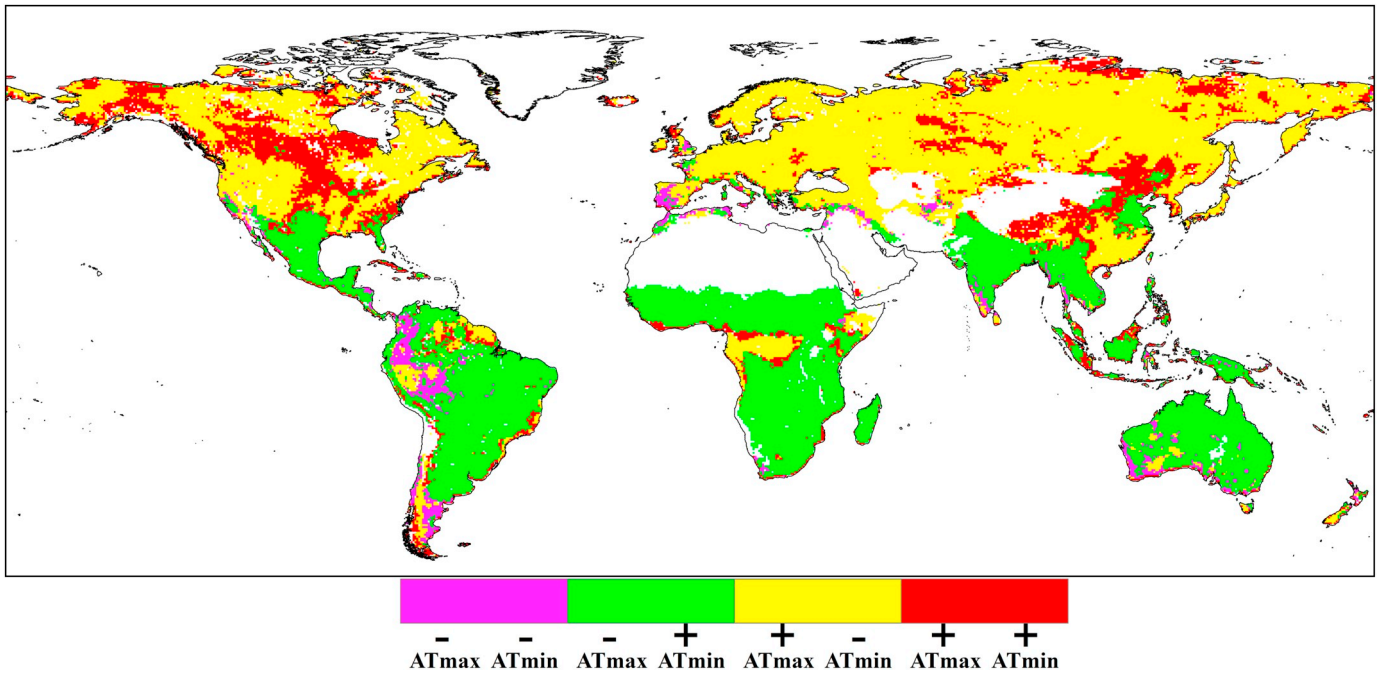

Fig. 3. Comparison of positive-negative aspects of OPR between NDVI and ATmax and ATmin. The plus sign refers to positive correlations, whereas the minus sign denotes negative correlations. The white areas represent places with no data or with no significant correlation ($p > .05$).

Fig. 3 collectively, we can see that the blue areas in Fig. 2.c incline to appear over the regions where the NDVI responds to both ATmax and ATmin positively (the red regions in Fig. 3) and negatively (the purple regions in Fig. 3), i.e., the northern Great Plains, some places on the Amazon Plain, the west Siberian Plain and the Mediterranean regions. However, the brown areas in Fig. 2.c tend to occur in the places covered by negative correlations between NDVI and ATmax and positive correlations between NDVI and ATmin (green regions in Fig. 3), i.e., the Greater Khingan Mountains, the Appalachian Mountains, the Brazil Plateau, and the Ronda and Katanga Plateau.

It can be seen from Fig. 4 (see also in Figs. S6 and S7) that the terrestrial vegetation types respond to both ATmax and ATmin with time-lag effects mostly ranging from 1 to 2 months, and the lagged time intervals for different vegetation types are unequal. Moreover, ATmin has the inclination to exhibit longer OTL on the NDVI in most vegetation types ATmax does. As shown in Fig. 4, the EBF (1.68 ± 1.19 months), followed by OShrub (1.65 ± 1.06 months), Crop (1.64 ± 0.95 months) and CShrub (1.55 ± 1.03 months), responds to ATmax with the longest prolonged duration; the lagged times of DBF (0.96 ± 0.75 months) and DNF (0.97 ± 0.18 months) responding to ATmax were very small. The ATmin has the longest asymmetric impacts on the DBF (1.78 ± 1.00 months), followed by EBF (1.73 ± 1.30 months), WoodG (1.79 ± 1.01 months) and OShrub (1.78 ± 1.10 months); meanwhile, the shortest lagged effects are exhibited in the responses of DNF (1.21 ± 0.60 months), ENF (1.37 ± 1.02 months) and MF (1.45 ± 0.92 months) to ATmin.

3.2. Partial correlations between NDVI and asymmetric warming

We obtained the OPR between NDVI and ATmax (Fig. 5.a) and ATmin (Fig. 5.b). Fig. 5.a (see also in Figs. S8.a and S9.a) shows that ATmax positively correlates with NDVI over the mid-high northern latitudes (> 45°N) and high elevations (i.e. the Tibetan Plateau); inversely, ATmax is negatively associated with NDVI over most of the other regions (with tropical places such as the Brazil Plateau, the Deccan Plateau and the African Sahel covered by the most intensively negative correlations). The patterns of the correlation between ATmin and NDVI (Fig. 5.b, Figs. S8.b and S9.b) are mostly the reverse of those between ATmax and NDVI; namely, they are positive over the arid regions and the majority of tropical regions (especially the Brazil Plateau, the Ronda and Katanga Plateau and the African Sahel) and negative over most of the mid-high northern latitudes (> 45°N) and some tropical rainforests, i.e., the Amazon and Congo Basin.

The probability densities of the OPR between NDVI and ATmax and ATmin across different vegetation types are shown in Figs. 6.a and b, respectively (see also Figs. S10.a-b and S11.a-b). A post hoc comparison shows that all pixels in DNF, and an overwhelming majority of grids of ENF (99.47%), followed by MF (95.44%) and Grass (78.60%), positively respond to ATmax, which results in the highest average OPR occur in these vegetation types; inversely, a dominant percentage (64.53%) of EBF pixels are negatively associated with ATmax, which causes EBF to have a negative average OPR in correlation with ATmax; however, the remaining vegetation types, show relatively even distributions of positive and negative correlations, and they correlate to ATmax with POR near zero. As for the correlations between NDVI and ATmin, the majority of pixels in DNF (98.56%), followed by MF (82.27%) and ENF (83.05%), are covered by negative values, which brings about the lowest average OPR in these vegetation types; however, the dominant EBF grids (65.86%) are dominated by positive correlations, which brings about the highest positive average OPR in EBF; and the other vegetation types are featured with near fifty-fifty distributions of positive and negative correlations with ATmin.

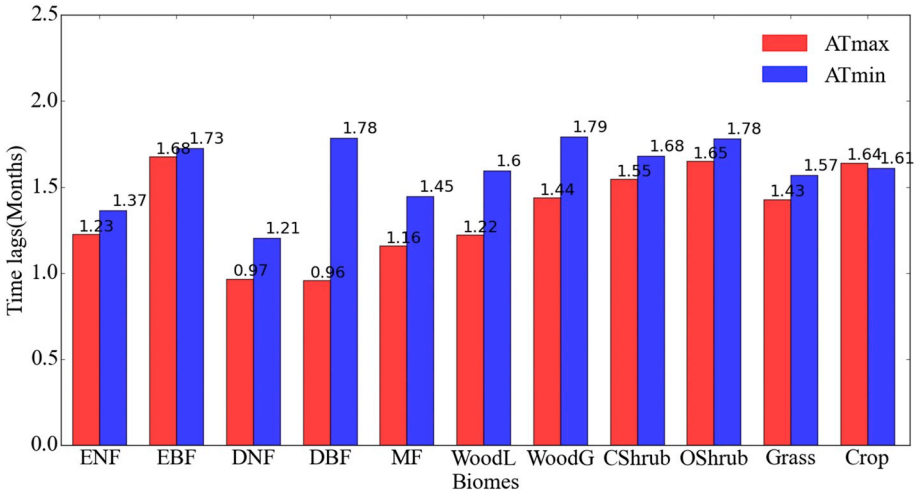

Fig. 4. The average OTL of NDVI responses to ATmax (red bars) and ATmin (blue bars) within different vegetation types. Only significant ($p \leq .05$) pixels are taken into consideration. Vegetation types are introduced in Fig. 1. (For interpretation of the references to colour in this figure legend, the reader is referred to the web version of this article.)

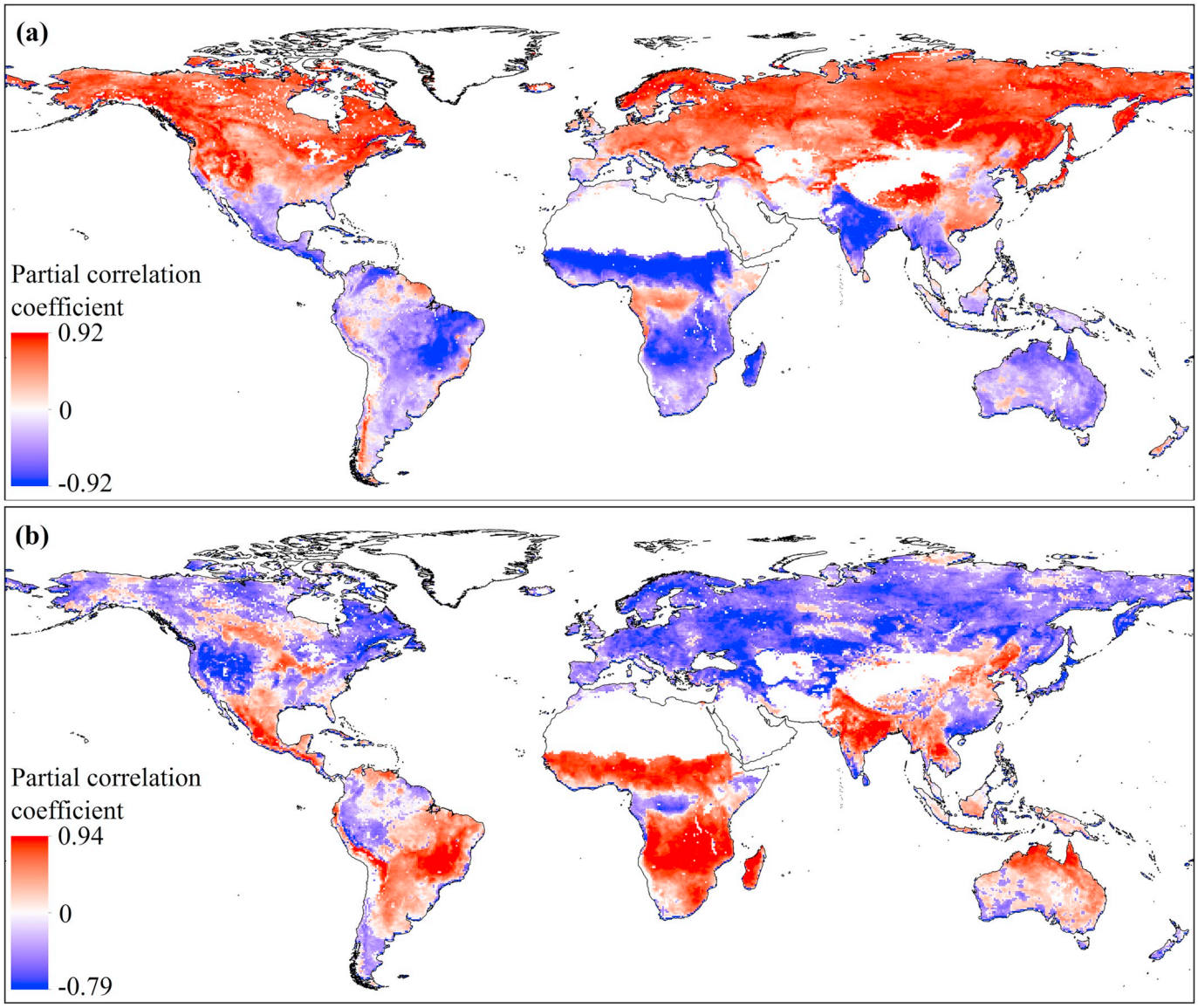

Fig. 5. Spatial distributions of OPR between NDVI and a) ATmax and b) ATmin from 1982 to 2014. The white areas represent places with no data or with no significant correlations ($p > .05$).

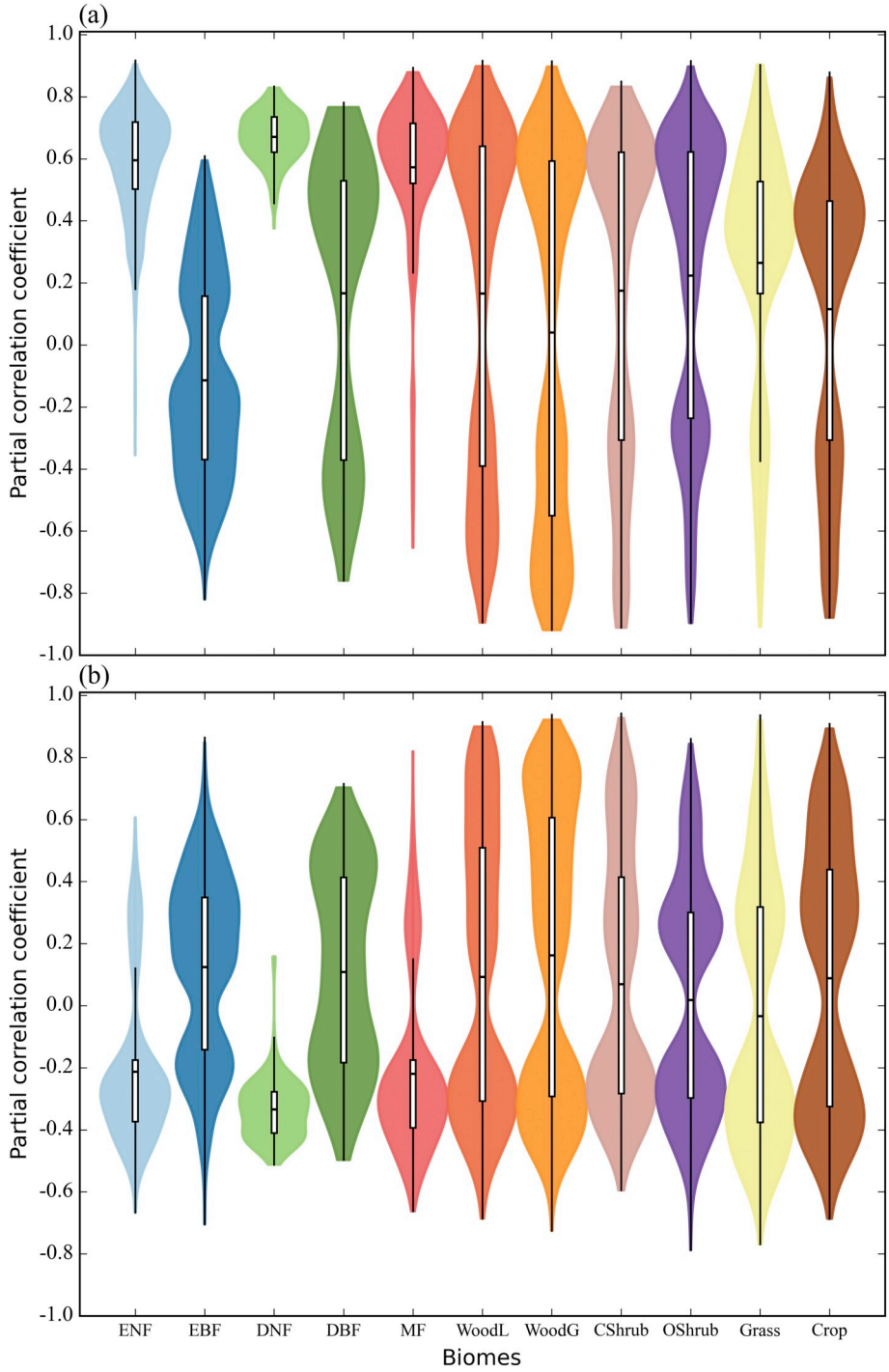

Fig. 6. Violin plots of OPR between NDVI and a) ATmax and b) ATmin within different vegetation types. The width of each violin plot represents the probability density of the partial correlation coefficient at different values. The inner horizontal line in each box represents the average correlation. This picture is related to Fig. 5 and only significant ($p \leq .05$) pixels are shown. The vegetation types are introduced in Fig. 1.

4. Discussion

The last 30-year has witnessed worldwide existence of asymmetric warming (Peng et al., 2013; Su et al., 2015; Tan et al., 2014). In this study, the variations in NDVI were used to indicate the changes in vegetation growth, and variations in ATmax and ATmin were used to reflect the asymmetric temperature warming trend in Tmax and Tmin, respectively. Unlike previous studies that mainly focus on the immediate effects of Tmax and/or Tmin on terrestrial vegetation, we quantitatively studied the inter-seasonal time-lag effects of Tmax and/or Tmin on vegetation growth by applying the partial correlation and time-lag analyses. The results confirmed our hypothesis that both Tmax and Tmin have significant, non-uniform time-lag effects on vegetation growth; Tmax and/or Tmin exhibit diverse time-lag impacts on different vegetation types; and the same vegetation type exhibits distinguishing asymmetric responses to Tmax vs. Tmin.

4.1. Time-lag effects of asymmetric warming on vegetation growth

Being unable to generate heat, green plants have to depend on ambient temperature as thermal energy to modulate the inner biogeochemical processes (Foote and Schaedle, 1976) and further regulate the

inter-seasonal growth and development. Previous researches have shown that the antecedent, ambient temperature has the most important impacts on the present vegetation growth (Mulder et al., 2016; Piao et al., 2003; Wu et al., 2015; Xu et al., 2014), which was confirmed again in the present study. Furthermore, our results suggested that Tmax vs. Tmin has unequal lagged effects on terrestrial vegetation growth across considerable terrestrial areas; the lag time intervals of the same type of vegetation in responding to Tmax vs. Tmin are not the same; and different plant types have unequal length of lagged duration in responding to Tmax and/or Tmin. These results are supported by previous studies (Braswell et al., 1997; Musau et al., 2016; Wu et al., 2015), which have also documented the distinguishing asymmetric responses of vegetation to ambient temperature over different spaces and vegetation types. The underling mechanisms behind these phenomena are to be discussed below.

The vegetation growth over high latitudes and altitudes is restricted predominantly to temperature (Nemani et al., 2003; Wu et al., 2015), and the inter-seasonal plant growth there is very sensitive to fluctuations in surrounding temperature (Tan et al., 2014), therefore, the vegetation have short time responses to asymmetric warming. The long lags in semi-arid and arid regions can be attributed to the mechanisms possessed by green plants that allow them to tolerate water shortages resulting from warming temperatures (Vicente-Serrano et al., 2013). These temperature and water related mechanisms may serve as the most pivotal role in accounting for the time-lag effects of asymmetric warming on NDVI.

Vegetation has different mechanisms in responding to the day-time and night-time temperature changes (Peng et al., 2013; Su et al., 2015; Tan et al., 2014), the unequal OTL of Tmax to Tmin on NDVI confirms this. First, the positive OTL differences (the blue areas in Fig. 2.c, Figs. S4.c and S5.c) mainly occur in regions where both Tmax and Tmin positively correlate with NDVI (the red regions areas in Fig. 3) and regions where both Tmax and Tmin negatively correlate with NDVI (the purple areas in Fig. 3). The red regions are mainly located in the high-latitude and high-elevation places (i.e., the Tibetan Plateau and some northern alpine regions) and predominantly covered by grass and crop, the plant growth there may require a relatively long time to store more energy from the sunlight during day-time photosynthesis to support growth and development under this cold ecosystems (Wan et al., 2009). They may have developed a mechanism to quickly respond to Tmin (Slot and Kitajima, 2015) in order to overcompensate for the negative effects from night-time respiration through strengthened day-time photosynthesis (Wan et al., 2009). Consequently, longer lagged duration exists in the NDVI responses to Tmax than to Tmin over the red regions. Second, most of the purple areas in Fig. 3 spread over the Mediterranean regions, where the warmer and drier weather makes drought a major limiting factor to the vegetation growth, and it's no surprise the NDVI is negatively correlated with both Tmax and Tmin. We suspected that there must exist adopted survival mechanisms that cause the Mediterranean plants to respond to Tmax with longer lagged interval than to Tmin, likely through their interactions with the variations in trace element and nutrient (Babst et al., 2013; Sardans et al., 2008) and the asymmetric diurnal variations in land surface temperature(He et al., 2017). Third, the negative OTL differences (the brown areas in Fig. 2.c, Figs. S4.c and S5.c) mainly occurs in the green areas in Fig. 3, which covers majorities of the tropical arid regions. The green plants there respond to Tmax quickly to cope with the suppressed growth rate from Tmax-introduced decreases in water availabilities (Anderegg et al., 2015); on the contrary, they respond to Tmin with a relatively long protracted duration, likely due to the respiration acclimation abilities (Atkin and Tjoelker, 2003; Slot and Kitajima, 2015), which allows green plants to acclimate to the Tmin and resist the passive impacts from Tmin on plants growth. Forth, Tmax tend to have equal OTL to Tmin (the pale yellow areas in Fig.2.c) over the regions where the overall absolute PR between NDVI and Tmax exhibits small difference (only 0.12) to that between NDVI and Tmin. This plausibly indicates that the vegetated regions with equal lagged time were tended to accompanied by equal correlation.

4.2. Correlations between asymmetric warming and vegetation growth

Tmax and Tmin can both enhance and suppress vegetation growth in opposite ways via different mechanisms (Peng et al., 2013). Vegetation growth in the mid-high northern latitudes and high elevations is predominantly restricted by temperature (Nemani et al., 2003; Wu et al., 2015). Tmax can significantly promote vegetation photosynthesis by making the day-time temperature approach the optimal temperature (Peng et al., 2013; Zhang et al., 2016); besides, Tmax can also positively correlate to vegetation growth through increasing the soil nitrogen mineralization and availability (Iii et al., 1995), elongating the plant growing season (Mulder et al., 2016; Piao et al., 2015) and enlarging the plant habitats poleward and uphill (Koven, 2013; Lenoir et al., 2008). Whereas, vegetation growth over the other regions, is mainly limited by precipitation and solar radiation (Nemani et al., 2003; Wu et al., 2015). Tmax tends to enhance the evaporation (Yan et al., 2013), reduce soil moisture and increase the soil drought conditions (Peng et al., 2013; Wan et al., 2009; Xia et al., 2014), which greatly precludes vegetation growth. Tmin has been reported to increase the dark respiration in plants (Anderegg et al., 2015; Peng et al., 2013), which is one of the main sources of carbon depletion in green plants; however, numerous recent studies have also found that increases in Tmin can facilitate vegetation growth by stimulation in the following-day carbon sequestration (Wan et al., 2009), elongation in plant growing season length (Piao et al., 2007), lessening in the risk from severe frost (Piao et al., 2015; Sherwood et al., 2017), increases in drought resistance abilities of plant communities (Yang et al., 2016) and enrichment of the soil nutrients (Phillips et al., 2016; Zhang et al., 2016). These mechanisms might, at least partly, help to explain the contrary spacial behaviors of NDVI correlated to Tmin.

The uniqueness of different plant types, i.e. the life form and structure, environmental adaption and morphological, biochemical, physiological and behavioral characteristics (Pan et al., 2013; Woodward et al., 2004; Xu et al., 2015), accounts for the distinguishing correlations between NDVI and Tmax and/or Tmin among different vegetation types. Living in the warm to cold climatic regions, the growth of ENF, DNF and MF are mainly restricted by temperature; Tmax can make diurnal temperature be closer to the optimal value for plant photosynthesis and further attribute the growth of these vegetation types (Chapin and Shaver, 1996; Zhou et al., 2003). On the contrary, the respiration of these vegetation types will also be enhanced by Tmin (Peng et al., 2013), which attenuates their growth rates. Therefore, these vegetation types were found to have dominant positive correlations with Tmax and negative correlations with Tmin. These mechanisms were supported by the results from Peng et al. (2013) and Tan et al. (2014). EBF presents predominant negative correlations with Tmax and the reverse is true for Tmin, which might be ascribed to the fact that EBF is habituated to tropical ecosystems, where increases in Tmax tends to increase the evaporation in soil, enhance the severity of drought and reduce the incoming solar radiation (Nemani et al., 2003; Wu et al., 2015), therefore, increases in Tmax is detrimental to the growth of EBF. On the contrary, increases in Tmin accelerates the litter decomposition and increases the nutrition availability in soil; this might be the most important reason that increases in Tmin attributes EBF growth (Phillips et al., 2016). These results were supported by the study by Musau et al. (2016), who also found similar complex responses of EBF to Tmax and Tmin in East Africa. Finally, three plant types, i.e., the C3, C4 and CAM, can be further classified in the remaining vegetation types (WoodL, WoodG, OShrub, CShrub, Grass and Crop), among which the C3 plants commonly grow in cold and wet habitats; however, the other two typically live in hot, sunny and dry habitats (Bareja, 2012; Woodward et al., 2004). Thus, higher temperature is good for the growth of C3 plants but bad for the other two types. These contrary

growing habits may critically, or at least partially, account for the complex correlations of these vegetation types with asymmetric warming (Braswell et al., 1997; Musau et al., 2016; Yamori et al., 2014).

4.3. Implications and uncertainties

The results of this study provide a new perspective on the responses of terrestrial vegetation to asymmetric warming, and our results highlight the necessity and significance of future studies and currently used climate-vegetation models to consider the non-uniform time-lag effects found in this study in order to better investigating the warming-vegetation interactions. There are very several significant ecological meanings that can be extracted from our results. For instance, combining the results in Figs. 4 and 6, we suggest that, given the background of increasing global warming, the inter-seasonal growth of ENF, DNF and MF tend to be positively and strongly affected by the conditions of previous Tmax, which lasts for ~1.12 months, but the growth of these vegetation types tends to be impacted by antecedent Tmin for ~1.34 months backwards; the majority of pixels of EBF were negatively associated with previous Tmax for ~ 1.68 months, and oppositely with earlier Tmin for ~1.73 months; as for Grass, dominant pixels in this vegetation type positively correlate with the condition of Tmax for ~1.43 months backwards, whereas, more than half of the Grass grids were negatively correlated with previous Tmin for ~1.57 months; the remaining vegetation types, however, were characterized by near fifty-fifty distributions of positive and negative correlations with both antecedent Tmax and Tmin for > 1 month. These distinguished results deserve to be considered and treated differently and carefully in monitoring and anticipating the variations of terrestrial vegetation responses to future asymmetric warming.

From the results of annual mean growing season length (Fig. S3), we can find decreasing trends from the equator to the poles, low elevations to high elevations, humid regions to arid regions (Julien and Sobrino, 2007). According to Fig. S12, the lagged time is larger than 1 month for each growing season, and it exhibits a decreasing trend for the growing season of 1 month to 6 months followed by an increasing trend still the growing season of 12 months ("V" shape for both Tmax and Tmin). From Fig. S13 we can found that Tmax positively correlated with vegetation growth at each length of growing season except the growing season of 12 months, and the correlation increased with the growing season rising from 1 to 6 months and decreased till 12 months ("∧" shape, Fig. S13.a). The correlations between Tmin and vegetation growth were almost the opposite ("V" shape, Fig. S13.b). These results showed that different lengths of growing season have significant impacts on the time-lag effects of asymmetric warming on vegetation growth. However, the reasons why "∧" and "V" shapes exhibited in the lagged time and correlations were uncertain, which calls for further researches to uncover the underlying mechanisms for how growing season affects time-lag effects.

Some limitations and uncertainties must also be recognized: (I) we focused on analyzing the responses of vegetation to climatic factors, while the impacts from non-climatic factors, i.e., human activities (such as changes in irrigation and fertilization practice and regular rotations cultivated types) (Rost et al., 2009; Tilman et al., 2002) and natural disturbances (such as wild fire hazard and pest outbreak) (Flower and Gonzalez-Meler, 2015; Verón et al., 2012) were not included. (II) We primarily focused on the geographical perspective in studying the time-lag effects of asymmetric warming on present vegetation growth, the underling biochemical mechanisms behind this non-uniform warming-induced time lags remains unclear. (III) The statistical analyses in this study were originally based on a linear regression model, thus the warming-driven effects on vegetation changes might be simplified to some extent. (IV) The present study was confined by the low spatial resolution data (0.5°), and finely spacial results for the growing season length, lagged time and correlations were not available, which would increase the uncertainties of this study inevitably. (V) The relationship between NDVI and many ecosystem properties, such as LAI and NPP etc., often get saturated when the surface vegetation cover reaches a certain high level, which is strongly related to the species of biomes (Zhang et al., 2000), vegetation growing seasons (Zhang et al., 2000) and spatial variations in environmental stress (Brantley et al., 2011). This paper is an exploratory research based on the NDVI, such that our analyses tended to be more sensitives in the regions and periods with low vegetation while less sensitives over others. Hence, additional researches about the time-lag impacts of Tmax and Tmin on vegetation growth remain to be shed light on, and incorporating better input data, integrating and combining the multi-model and various-study results might be greatly helpful.

5. Conclusions

In summary, we investigated the inter-seasonal, non-uniform time-lag effects of terrestrial vegetation responses to asymmetrical warming from 1982 to 2014. Key findings are drawn as follows: on the one hand, the inter-seasonal growth of terrestrial vegetation responds to Tmax and Tmin with an overall average time lag of 1.68 ± 1.05 months and 1.45 ± 0.96 months, respectively; these time lags are distributed heterogeneously across spaces, with smaller values distributing over temperature-limited regions and larger values over other places, particularly the arid regions; considerable amounts (43.44%) of vegetation pixels have unequal time lags in responding to Tmax than to Tmin; the average time lags for different vegetation types mostly range between ~1–2 months, with longer lagged time resulted from Tmin than from Tmax. On the other hand, the Tmax positively correlates with NDVI over the mid-high northern latitudes and high altitudes and is negatively associated with NDVI over most of the remaining regions; the patterns of the correlations between Tmin and NDVI are mostly the reverse of that between Tmax and NDVI; furthermore, the vegetation species of DNF, ENF, MF and Grass tend to positively respond to Tmax but negatively respond to Tmin; however, the remaining vegetation types are featured with near fifty-fifty distributions of positive and negative correlations with Tmax and Tmin. The different mechanisms of day-time and night-time temperature on vegetation and the uniqueness of different plant types account for these results; however, additional research is needed to better understand the mechanisms behind these phenomena.

Acknowledgments

This work was funded by the National Key R & D Program of China (No. 2017YFA0604404), the Key National Natural Science Foundation of China (Grant No. 41531176), and the National Natural Science Foundation of China (Grant No. 41671398).

Appendix A. Supplementary data

Supplementary data to this article can be found online at https://doi.org/10.1016/j.gloplacha.2019.03.010.

References

Anandhi, A., 2016. Growing degree days – Ecosystem indicator for changing diurnal temperatures and their impact on corn growth stages in Kansas. Ecol. Indic. 61, 149–158. https://doi.org/10.1016/j.ecolind.2015.08.023.

Anderegg, W.R.L., Ballantyne, A.P., Smith, W.K., Majkut, J., Rabin, S.S., Beaulieu, C., Birdsey, R., Dunne, J.P., Houghton, R.A., Myneni, R.B., Pan, Y., Sarmiento, J.L., Serota, N., Shevliakova, E., Tan, P., Pacala, S.W., 2015. Tropical nighttime warming as a dominant driver of variability in the terrestrial carbon sink. Proc. Natl. Acad. Sci. U. S. A. 112 (51). https://doi.org/10.1073/pnas.1521479112.

Atkin, O.K., Tjoelker, M.G., 2003. Thermal acclimation and the dynamic response of plant respiration to temperature. Trends Plant Sci. 8 (7), 343–351. https://doi.org/10.1016/S1360-1385(03)00136-5.

Babst, F., Poulter, B., Trouet, V., Tan, K., Neuwirth, B., Wilson, R., Carrer, M., Grabner,

M., Tegel, W., Levanic, T., Panayotov, M., Urbinati, C., Bouriaud, O., Ciais, P., Frank, D., 2013. Site- and species-specific responses of forest growth to climate across the European continent. Glob. Ecol. Biogeogr. 22 (6), 706–717. https://doi.org/10.1111/geb.12023.

Bareja, B.G., 2012. The History of Photosynthesis: Contributions of Early Researchers. Retrieved < 5-15-2017 > from. http://www.cropsreview.com/history-of-photosynthesis.html.

Brantley, S.T., Zinnert, J.C., Young, D.R., 2011. Application of hyperspectral vegetation indices to detect variations in high leaf area index temperate shrub thicket canopies. Remote Sens. Environ. 115 (2), 514–523. https://doi.org/10.1016/j.rse.2010.09.020.

Braswell, B.H., Schimel, D.S., Linder, E., Moore, B., 1997. The response of global terrestrial ecosystems to interannual temperature variability. Science 278 (278), 870–873. https://doi.org/10.1126/science.278.5339.870.

Chapin, F.S., Shaver, G.R., 1996. Physiological and growth responses of Arctic plants to a field experiment simulating climatic change. Ecology 77, 822–840. https://doi.org/10.2307/2265504.

Chen, B., Gao, Y., Liao, H., Peng, S., 2017. Differential responses of invasive and native plants to warming with simulated changes in diurnal temperature ranges. AoB Plants 9https://doi.org/10.1093/aobpla/plx028. plx028-plx028.

Defries, R.S., Hansen, M.C., 2010. ISLSCP II University of Maryland Global Land Cover Classifications, 1992–1993. ORNL Distributed Active Archive Center.

Dutta, D., Kundu, A., Patel, N.R., Saha, S.K., Siddiqui, A.R., 2015. Assessment of agricultural drought in Rajasthan (India) using remote sensing derived Vegetation Condition Index (VCI) and standardized Precipitation Index (SPI). Egypt. J. Remote Sens. Space Sci. 18, 53–63. https://doi.org/10.1016/j.ejrs.2015.03.006.

Eidenshink, J.C., Faundeen, J.L., 1994. The 1 km AVHRR global land data set: first stages in implementation. Int. J. Remote Sens. 15 (17), 3443–3462. https://doi.org/10.1080/01431169408954339.

Flower, C.E., Gonzalez-Meler, M.A., 2015. Responses of temperate forest productivity to insect and pathogen disturbances. Annu. Rev. Plant Biol. 66, 547–569. https://doi.org/10.1146/annurev-arplant-043014-115540.

Foote, K.C., Schaedle, M., 1976. Physiological characteristics of photosynthesis and respiration in stems of Populus tremuloides Michx. Plant Physiol. 58 (1), 91–94. https://doi.org/10.2307/4264498.

Garcia-Mozo, H., Galan, C., Gomez-Casero, M.T., Dominguez, E., 2000. A comparative study of different temperature accumulation methods for predicting the start of the Quercus pollen season in Cordoba (South West Spain). Grana 39, 194–199. https://doi.org/10.1080/00173130051084322.

Gordon, J., 2008. Asymmetric variability between maximum and minimum temperatures in Northeastern Tibetan Plateau:evidence from tree rings. Sci. China Earth Sci. 51 (1), 41–55. https://doi.org/10.1007/s11430-007-0154-1.

Hansen, M.C., Defries, R.S., Townshend, J.R.G., Sohlberg, R., 2000. Global land cover classification at 1 km spatial resolution using a classification tree approach. Int. J. Remote Sens. 21 (6–7), 1331–1364. https://doi.org/10.1080/014311600210209.

Harris, I., Jones, P.D., Osborn, T.J., Lister, D.H., 2014. Updated high-resolution grids of monthly climatic observations – the CRU TS3.10 Dataset. Int. J. Climatol. 34 (3), 623–642. https://doi.org/10.1002/joc.3711.

He, B., Huang, L., Liu, J., Wang, H., Lǚ, A., Jiang, W., Chen, Z., 2017. The observed cooling effect of desert blooms based on high-resolution Moderate Resolution Imaging Spectroradiometer products. Earth Space Sci. 4 (5), 247–256. https://doi.org/10.1002/2016EA000238.

Iii, F.S.C., Shaver, G.R., Giblin, A.E., 1995. Responses of Arctic Tundra to experimental and observed changes in climate. Ecology 76 (3), 694–711.

IPCC, 2014. In: Core Writing Team, Pachauri, R.K., Meyer, L.A. (Eds.), Climate Change 2014: Synthesis Report. Contribution of Working Groups I, II and III to the Fifth Assessment Report of the Intergovernmental Panel on Climate Change. IPCC, Geneva, Switzerland (151 pp.).

Julien, Y., Sobrino, J.A., 2007. Changes in the global vegetal cover through a phenological analysis of GIMMS data. In: Paper presented at the 2007 International Workshop on the Analysis of Multi-temporal Remote Sensing Images.

Koven, C.D., 2013. Boreal carbon loss due to poleward shift in low-carbon ecosystems. Nat. Geosci. 6 (6), 452–456. https://doi.org/10.1038/ngeo1801.

Lenoir, J., Gégout, J.C., Marquet, P.A., De, R.P., Brisse, H., 2008. A significant upward shift in plant species optimum elevation during the 20th century. Science 320 (5884), 1768. https://doi.org/10.1126/science.1156831.

Mulder, C.P.H., Iles, D.T., Rockwell, R.F., 2016. Increased variance in temperature and lag effects alter phenological responses to rapid warming in a subarctic plant community. Glob. Chang. Biol. 23 (2), 801–814. https://doi.org/10.1111/gcb.13386.

Musau, J., Patil, S., Sheffield, J., Marshall, M., 2016. Spatio-temporal vegetation dynamics and relationship with climate over East Africa. Hydrol. Earth Syst. Sci. Discuss. 1–30. https://doi.org/10.5194/hess-2016-502.

Nemani, R.R., Keeling, C.D., Hashimoto, H., Jolly, W.M., Piper, S.C., Tucker, C.J., Myneni, R.B., Running, S.W., 2003. Climate-driven increases in global terrestrial net primary production from 1982 to 1999. Science 300 (5625), 1560–1563. https://doi.org/10.1126/science.1082750.

Pan, Y., Birdsey, R.A., Phillips, O.L., Jackson, R.B., 2013. The structure, distribution, and biomass of the world's forests. Ann. Rev. Ecol. Evol. Syst. 44 (44), 593–622. https://doi.org/10.1146/annurev-ecolsys-110512-135914.

Peng, D., Huang, J., Huete, A., Yang, T., Gao, P., Chen, Y., Chen, H., Li, J., Liu, Z., 2010. Spatial and seasonal characterization of net primary productivity and climate variables in southeastern China using MODIS data. J. Zhejiang Univ. 11 (4), 275–285. https://doi.org/10.1631/jzus.b0910501.

Peng, S., Piao, S., Ciais, P., Myneni, R., Chen, A., Chevallier, F., Dolman, A.J., Janssens, I.A., Peñuelas, J., Zhang, G., Vicca, S., Wan, S., Wang, S., Zeng, H., 2013. Asymmetric effects of daytime and night-time warming on Northern Hemisphere vegetation. Nature 501 (7465), 88. https://doi.org/10.1038/nature12434.

Phillips, C.L., Murphey, V., Lajtha, K., Gregg, J.W., 2016. Asymmetric and symmetric warming increases turnover of litter and unprotected soil C in grassland mesocosms. Biogeochemistry 128 (1), 217–231. https://doi.org/10.1007/s10533-016-0204-x.

Piao, S., Fang, J., Zhou, L., Guo, Q., Henderson, M., Ji, W., Li, Y., Tao, S., 2003. Interannual variations of monthly and seasonal normalized difference vegetation index (NDVI) in China from 1982 to 1999. J. Geophys. Res. Atmos. 108, 4401. https://doi.org/10.1029/2002JD002848.

Piao, S., Friedlingstein, P., Ciais, P., Viovy, N., Demarty, J., 2007. Growing season extension and its impact on terrestrial carbon cycle in the Northern Hemisphere over the past 2 decades. Glob. Biogeochem. Cycles 21 (3). https://doi.org/10.1029/2006GB002888. (GB3018).

Piao, S., Tan, J., Chen, A., Fu, Y.H., Ciais, P., Liu, Q., Janssens, I.A., Vicca, S., Zeng, Z., Jeong, S.J., Li, Y., Myneni, R.B., Peng, S., Shen, M., Penuelas, J., 2015. Leaf onset in the northern hemisphere triggered by daytime temperature. Nat. Commun. 6, 6911. https://doi.org/10.1038/ncomms7911.

Potter, C.S., Klooster, S., Genovese, V., 2012. Net primary production of terrestrial ecosystems from 2000 to 2009. Clim. Chang. 115 (2), 365–378. https://doi.org/10.1007/s10584-012-0460-2.

Rost, S., Gerten, D., Hoff, H., Lucht, W., Falkenmark, M., 2009. Global potential to increase crop production through water management in rainfed agriculture. Environ. Res. Lett. 4 (4). https://doi.org/10.1088/1748-9326/4/4/044002. (044002).

Sardans, J., Peñuelas, J., Estiarte, M., 2008. Warming and drought change trace element bioaccumulation patterns in a Mediterranean shrubland. Chemosphere 70 (5), 874–885. https://doi.org/10.1016/j.chemosphere.2007.06.085.

Sheffield, J., Goteti, G., Wood, E.F., 2006. Development of a 50-year high-resolution global dataset of meteorological forcings for land surface modeling. J. Clim. 19, 3088–3111. https://doi.org/10.1175/jcli3790.1.

Shen, X., Liu, B., Zhou, D., 2015. Using GIMMS NDVI time series to estimate the impacts of grassland vegetation cover on surface air temperatures in the temperate grassland region of China. Remote Sens. Lett. 7 (3), 229–238. https://doi.org/10.1080/2150704x.2015.1128131.

Sherry, R.A., Weng, E., Arnone Iii, J.A., Johnson, D.W., Schimel, D.S., Verburg, P.S., Wallace, L.L., Luo, Y., 2008. Lagged effects of experimental warming and doubled precipitation on annual and seasonal aboveground biomass production in a tallgrass prairie. Glob. Chang. Biol. 14, 2923–2936. https://doi.org/10.1111/j.1365-2486.2008.01703.x.

Sherwood, J.A., Debinski, D.M., Caragea, P.C., Germino, M.J., 2017. Effects of experimentally reduced snowpack and passive warming on montane meadow plant phenology and floral resources. Ecosphere 8https://doi.org/10.1002/ecs2.1745. (e01745).

Slot, M., Kitajima, K., 2015. General patterns of acclimation of leaf respiration to elevated temperatures across biomes and plant types. Oecologia 177 (3), 885. https://doi.org/10.1007/s00442-014-3159-4.

Su, H., Feng, J., Axmacher, J.C., Sang, W., 2015. Asymmetric warming significantly affects net primary production, but not ecosystem carbon balances of forest and grassland ecosystems in northern China. Sci. Rep. 5, 9115. https://doi.org/10.1038/srep09115.

Tan, J., Piao, S., Chen, A., Zeng, Z., Ciais, P., Janssens, I.A., Mao, J., Myneni, R., Peng, S., Peñuelas, J., Shi, X., Vicca, S., 2014. Seasonally different response of photosynthetic activity to daytime and night-time warming in the Northern Hemisphere. Glob. Chang. Biol. 21 (1), 377. https://doi.org/10.1111/gcb.12724.

Tilman, D., Cassman, K.G., Matson, P.A., Naylor, R., Polasky, S., 2002. Agricultural sustainability and intensive production practices. Nature 418, 671. https://doi.org/10.1038/nature01014.

Tucker, C.J., Pinzon, J.E., Brown, M.E., Slayback, D.A., Pak, E.W., Mahoney, R., Vermote, E.F., El Saleous, N., 2005. An extended AVHRR 8-km NDVI dataset compatible with MODIS and SPOT vegetation NDVI data. Int. J. Remote Sens. 26 (20), 4485–4498. https://doi.org/10.1080/01431160500168686.

Turner, D.P., Ritts, W.D., Cohen, W.B., Gower, S.T., Running, S.W., Zhao, M., Costa, M.H., Kirschbaum, A.A., Ham, J.M., Saleska, S.R., Ahl, D.E., 2006. Evaluation of MODIS NPP and GPP products across multiple biomes. Remote Sens. Environ. 102 (3), 282–292. https://doi.org/10.1016/j.rse.2006.02.017.

Verón, S.R., Jobbágy, E.G., Bella, C.M.D., Paruelo, J.M., Jackson, R.B., 2012. Assessing the potential of wildfires as a sustainable bioenergy opportunity. Global Change Biol. Bioenergy 4 (6), 634–641. https://doi.org/10.1111/j.1757-1707.2012.01181.x.

Vicente-Serrano, S.M., Gouveia, C., Camarero, J.J., Beguería, S., Trigo, R., López moreno, J.I., Azorínmolina, C., Pasho, E., Lorenzolacruz, J., Revuelto, J., 2013. Response of vegetation to drought time-scales across global land biomes. Proc. Natl. Acad. Sci. U. S. A. 110, 52–57. https://doi.org/10.1073/pnas.1207068110.

Vose, R.S., Easterling, D.R., Gleason, B., 2005. Maximum and minimum temperature trends for the globe: an update through 2004. Geophys. Res. Lett. 32 (23). https://doi.org/10.1029/2005GL024379. (L23822).

Wan, S., Xia, J., Liu, W., Niu, S., 2009. Photosynthetic overcompensation under nocturnal warming enhances grassland carbon sequestration. Ecology 90 (10), 2700.

Wang, W., Anderson, B.T., Entekhabi, D., Huang, D., Su, Y., Kaufmann, R.K., Myneni, R.B., 2009. Intraseasonal interactions between temperature and vegetation over the boreal forests. Earth Interact. 11, 363–379. https://doi.org/10.1175/EI219.1.

Wang, X., Gao, Q., Wang, C., Yu, M., 2017. Spatiotemporal patterns of vegetation phenology change and relationships with climate in the two transects of East China. Global Ecol. Conserv. 10, 206–219. https://doi.org/10.1016/j.gecco.2017.01.010.

Weber, R.O., Talkner, P., Stefanicki, G., 1994. Asymmetric diurnal temperature change in the Alpine Region. Geophys. Res. Lett. 21 (8), 673–676. https://doi.org/10.1029/94GL00774.

Wiegand, T., Snyman, H.A., Kellner, K., Paruelo, J.M., 2004. Do grasslands have a memory: modeling phytomass production of a semiarid South African grassland.

Ecosystems 7, 243–258. https://doi.org/10.1007/s10021-003-0235-8.
Woodward, F.I., Lomas, M.R., Kelly, C.K., 2004. Global climate and the distribution of plant biomes. Philos. Transac. R. Soc. B Biol. Sci. 359 (1450), 1465. https://doi.org/10.1098/rstb.2004.1525.
Wu, D., Zhao, X., Liang, S., Zhou, T., Huang, K., Tang, B., Zhao, W., 2015. Time-lag effects of global vegetation responses to climate change. Glob. Chang. Biol. 21 (9), 3520–3531. https://doi.org/10.1111/gcb.12945.
Xia, J., Wan, S., 2012. The effects of warming-shifted plant phenology on ecosystem carbon exchange are regulated by precipitation in a semi-arid grassland. PLoS One 7https://doi.org/10.1371/journal.pone.0032088. (e32088).
Xia, J., Chen, J., Piao, S., Ciais, P., Luo, Y., Wan, S., 2014. Terrestrial carbon cycle affected by non-uniform climate warming. Nat. Geosci. 7 (3), 173–180. https://doi.org/10.1038/ngeo2093.
Xu, G., Zhang, H., Chen, B., Zhang, H., Innes, J., Wang, G., Yan, J., Zheng, Y., Zhu, Z., Myneni, R., 2014. Changes in vegetation growth dynamics and relations with climate over China's landmass from 1982 to 2011. Remote Sens. 6 (4), 3263–3283. https://doi.org/10.3390/rs6043263.
Xu, L., Saatchi, S.S., Yang, Y., Myneni, R.B., Frankenberg, C., Chowdhury, D., Bi, J., 2015. Satellite observation of tropical forest seasonality: spatial patterns of carbon exchange in Amazonia. Environ. Res. Lett. 10 (8). https://doi.org/10.1088/1748-9326/10/8/084005.
Yamori, W., Hikosaka, K., Way, D.A., 2014. Temperature response of photosynthesis in C3, C4, and CAM plants: temperature acclimation and temperature adaptation. Photosynth. Res. 119 (1), 101–117. https://doi.org/10.1007/s11120-013-9874-6.
Yan, H., Yu, Q., Zhu, Z., Myneni, R.B., Yan, H., Wang, S., Shugart, H.H., 2013. Diagnostic analysis of interannual variation of global land evapotranspiration over 1982–2011: assessing the impact of ENSO. J. Geophys. Res.-Atmos. 118 (16), 8969–8983. https://doi.org/10.1002/jgrd.50693.
Yang, Z., Zhang, Q., Su, F., Zhang, C., Pu, Z., Xia, J., Wan, S., Jiang, L., 2016. Daytime warming lowers community temporal stability by reducing the abundance of dominant, stable species. Glob. Chang. Biol. 23 (1), 154–163. https://doi.org/10.1111/gcb.13391.
Zeng, F., Collatz, G.J., Pinzon, J.E., Ivanoff, A., 2013. Evaluating and quantifying the climate-driven interannual variability in Global Inventory Modeling and Mapping Studies (GIMMS) normalized difference vegetation index (NDVI3g) at global scales. Remote Sens. 5, 3918–3950. https://doi.org/10.3390/rs5083918.
Zhang, Y., Tian, Y., Knyazikhin, Y., Martonchik, J.V., Diner, D.J., Leroy, M., Myneni, R.B., 2000. Prototyping of MISR LAI and FPAR algorithm with POLDER data over Africa. IEEE Trans. Geosci. Remote Sens. 38 (5), 2402–2418. https://doi.org/10.1109/36.868895.
Zhang, T., Xu, M., Xi, Y., Zhu, J., Tian, L., Zhang, X., Wang, Y., Li, Y., Shi, P., Yu, G., 2015. Lagged climatic effects on carbon fluxes over three grassland ecosystems in China. J. Plant Ecol. 8 (3), 291–302. https://doi.org/10.1093/jpe/rtu026.
Zhang, T., Yang, S., Guo, R., Guo, J., 2016. Correction: Warming and nitrogen addition alter photosynthetic pigments, sugars and nutrients in a temperate meadow ecosystem. PLoS One 11https://doi.org/10.1371/journal.pone.0158249. (e0158249).
Zhou, L., Kaufmann, R.K., Tian, Y., Myneni, R.B., Tucker, C.J., 2003. Relation between interannual variations in satellite measures of northern forest greenness and climate between 1982 and 1999. J. Geophys. Res. Atmos. 108 (D1). https://doi.org/10.1029/2002jd002510. ACL 3-1–ACL 3-16.
Zhou, L., Dickinson, R.E., Dirmeyer, P., Dai, A., Min, S.K., 2009. Spatiotemporal patterns of changes in maximum and minimum temperatures in multi-model simulations. Geophys. Res. Lett. 36 (2), 206–218. https://doi.org/10.1029/2008GL036141.
Zhu, Z., Bi, J., Pan, Y., Ganguly, S., Anav, A., Xu, L., Samanta, A., Piao, S., Nemani, R., Myneni, R., 2013. Global data sets of vegetation leaf area index (LAI)3g and fraction of photosynthetically active radiation (FPAR)3g derived from global inventory modeling and mapping studies (GIMMS) normalized difference vegetation index (NDVI3g) for the period 1981 to 2011. Remote Sens. 5 (2), 927–948. https://doi.org/10.3390/rs5020927.